Geophys. J. Int. (2002) **149,** 1–14

Seismic anisotropy and mantle creep in young orogens

Rolf Meissner,[1,2] Walter D. Mooney[2] and Irina Artemieva[3]

[1] *Institute for Geoscience, Kiel University,* D-24118 *Kiel, Germany*
[2] *US Geological Survey, MS 977 Menlo Park,* CA 94025, *USA*
[3] *Department of Earth Sciences, Uppsala University,* S-75236 *Uppsala, Sweden*

Accepted 2001 August 8. Received 2001 July 30; in original form 2000 July 7

SUMMARY

Seismic anisotropy provides evidence for the physical state and tectonic evolution of the lithosphere. We discuss the origin of anisotropy at various depths, and relate it to tectonic stress, geotherms and rheology. The anisotropy of the uppermost mantle is controlled by the orthorhombic mineral olivine, and may result from ductile deformation, dynamic recrystallization or annealing. Anisotropy beneath young orogens has been measured for the seismic phase *Pn* that propagates in the uppermost mantle. This anisotropy is interpreted as being caused by deformation during the most recent thermotectonic event, and thus provides information on the process of mountain building. Whereas tectonic stress and many structural features in the upper crust are usually orientated perpendicular to the structural axis of mountain belts, *Pn* anisotropy is aligned parallel to the structural axis. We interpret this to indicate mountain-parallel ductile (i.e. creeping) deformation in the uppermost mantle that is a consequence of mountain-perpendicular compressive stresses. The preferred orientation of the fast axes of some anisotropic minerals, such as olivine, is known to be in the creep direction, a consequence of the anisotropy of strength and viscosity of orientated minerals. In order to explain the anisotropy of the mantle beneath young orogens we extend the concept of crustal 'escape' (or 'extrusion') tectonics to the uppermost mantle. We present rheological model calculations to support this hypothesis. Mountain-perpendicular horizontal stress (determined in the upper crust) and mountain-parallel seismic anisotropy (in the uppermost mantle) require a zone of ductile decoupling in the middle or lower crust of young mountain belts. Examples for stress and mountain-parallel *Pn* anisotropy are given for Tibet, the Alpine chains, and young mountain ranges in the Americas. Finally, we suggest a simple model for initiating mountain parallel creep.

Key words: anisotropy, coupling, creep, rheology, tectonic escape.

INTRODUCTION

Seismic anisotropy is a characteristic property of large parts of the crust and upper mantle. It is caused by several factors, such as: (1) fine-scale layering of isotropic layers with velocity contrasts (Backus 1962; Helbig 1984); (2) cracks and fractures aligned in a preferred direction (Crampin 1984, 1989); and (3) strain-induced orientation of anisotropic minerals, such as biotite and hornblende in the crust, and olivine and pyroxene in the upper mantle (Babuska 1981; Mainprice & Nicolas 1989; Babuska & Cara 1991). There is a wealth of papers on seismic anisotropy, and we summarize the most important results in Table 1. Theoretical studies define anisotropy as direction dependence of a physical property such as the elastic tensor. For practical purposes we calculate seismic anisotropy according to Kern & Richter (1981)

$$A = (V_{\max} - V_{\min})/V_{\max} \text{ (in per cent)}, \quad (1)$$

where $V_{\max}$ and $V_{\min}$ are the maximum and minimum seismic velocities, respectively.

Most observations of seismic anisotropy distinguish between azimuthal and transverse anisotropy. Azimuthal anisotropy describes wave propagation that depends on the azimuth of propagation in the horizontal plane (Babuska & Cara 1991); the term transverse anisotropy was originally introduced by Love (1927) and describes a medium with one axis of cylindrical symmetry, which is equivalent to hexagonal symmetry for seismic wave propagation. Azimuthal anisotropy has been observed on seismic refraction profiles recorded at different azimuths (Bamford 1977) and by the splitting of vertically arriving *S* waves (Vinnik *et al.* 1992; Silver 1996; Savage 1999). Transverse anisotropy is observed by travel-time differences between *SV* and *SH* waves, or by differences in the dispersion of Love and Rayleigh waves (Montagner & Nataf 1986; Anderson 1989; Montagner 1998; Ekström & Dziewonski 1998).

Table 1. Overview of causes of seismic anisotropy.

Causes of anisotropy	Where?
(1) Periodic layering of isotropic layers of contrasting velocity and small thickness $d \ll \lambda$, creating transverse anisotropy, d = layer thickness; λ = seismic wavelength	In sediments and warm lower crust $V_x \cong V_y > V_z$ $V = P$-Wave velocity $v_x^{(SH)} > v_y^{(SH)} > v_z^{(SV)}$ $v = S$-Wave velocity $v_z^{(SH)} \cong v_z^{(SV)}$
(2) Aligned microcracks and fractures in the x-z-plane, creating azimuthal and transverse anisotropy	In sediments and upper crystalline crust $V_x \cong V_z > V_y$; $v_z^{(x)} > v_z^{(y)}$; $v_y^{(SH)} \cong v_x^{(SV)}$; $v_x^{(SH)} < v_y^{(SV)}$
(3) Lattice preferred orientation (LPO) (in x) (aligned anisotropic minerals), strain induced, creating azimuthal and transverse anisotropy	In warm lower crust and in the upper mantle and possibly in the asthenosphere $V_x > V_z >= V_y$
(4) Apparent (geometrical) anisotropy due to orientated inclusions with different velocity than in the surrounding	Probably in the lower crust and upper mantle

References: (1) Helbig (1984); Weiss *et al.* (1999); (2) Crampin (1984, 1989); Kern *et al.* (1996); (3) Ribe (1989); Savage (1999); (4) Siegesmund (1996); Budsansky & O'Connel (1976).

Seismic anisotropy has been observed in many parts of the crust and upper mantle (Anderson 1989; Babuska & Cara 1991; Plomerová *et al.* 1998), from the continental upper crust (Jones & Nur 1984; Kern *et al.* 1996), lower crust (Rabbel & Mooney 1996), subcrustal lithosphere and asthenosphere (Bamford 1977; Leven *et al.* 1981; Vinnik *et al.* 1992; Montagner 1998). It is often difficult, particularly using vertically arriving *S* waves, to uniquely determine the depth (or depths, in the case of multiple layers) of anisotropy. For this reason, methods that exploit *Pn* traveltime data to measure azimuthal anisotropy in the upper tens of kilometres below the Moho are particularly useful. These methods have the distinct advantage of constraining the depth of the anisotropic layer, in contrast with methods that utilize teleseismic data (Silver 1996; Savage 1999). It is well known (Bamford 1977; Fowler 1990) that *Pn* waves in nature are not simple head waves on top of the mantle but they slightly dive into the uppermost mantle under the influence of a small velocity gradient zone, showing a very small curvature in a traveltime diagram.

Interpretation of *Pn* is often hindered by a trade-off between heterogeneity and anisotropy (Tommasi *et al.* 1999), a problem that can be solved by reverse shooting or by using multiple-direction seismological observations. The latter method was refined by Smith & Ekström (1999) using a data set from the International Seismological Centre, selecting only continuous *Pn* data up to several 100 km distance and a refined processing methods to avoid errors from Moho dip and heterogeneity. In this way they were able to obtain good anisotropy estimates for more than 200 geographically distributed areas for the shallow mantle.

Another important branch of anisotropy studies are laboratory experiments of xenolith samples from various parts of the lithosphere. Natural (and artificial) samples have been investigated under appropriate pressure–temperature conditions (Kern *et al.* 1996; Ji *et al.* 1994). These experiments determine the deformation and the local directional dependence of seismic velocity, i.e. the anisotropy of the sample. Often they agree with the field data, but sometimes their extrapolation to long-wavelength seismological data is problematic (Babuska & Cara 1991). Based on a large number of naturally (and experimentally) deformed peridotitic samples the strain and stress that caused the specific deformation has been calculated for a viscoplastic model (Tommasi *et al.* 1999) and even the observed recrystallization has been taken into account (Wenk & Tomé 1999).

We discuss the origin of anisotropy in the crust and uppermost mantle in terms of processes that are controlled by temperature, rheology, and deformation. We disregard anisotropy within sedimentary basins (Helbig 1984) and concentrate on anisotropy owing to the lattice preferred orientation (LPO) of anisotropic minerals (Table 1). In our discussion of the relationship between anisotropy and tectonics we focus on young mountain belts that have thick crustal roots and high geothermal gradients. They are 'heating events' (Silver 1996). These orogens generally have *Pn* anisotropy with the fast direction orientated parallel to the structural axis, i.e. mountain-parallel (Smith & Ekström 1999). We notice that anisotropy from *S*-wave splitting and tectonic movement parallel to orogenic belts was already observed by Vauchez & Nicolas (1991) and Tommasi *et al.* (1999). We will review their explanation later.

We compare the orientation of *Pn* anisotropy with the direction of compressive stress, which nearly always shows a mountain-perpendicular component in the upper crust (Zoback 1992). From the discrepancy of directions between the fast axis of mantle anisotropy and the compressive crustal stresses we therefore postulate, in agreement with earlier suggestions (Sibson 1982; Meissner & Strehlau 1982), the existence of a decoupling layer. This layer is generally found in the middle or lower crust in all areas with high geothermal gradients and especially in young and warm mountain belts. A decoupling layer such as this corresponds to a low-viscosity layer capable of creep owing to tectonic stress. The weak layer in the crust will facilitate the process of tectonic escape, as described by Burke & Sengör (1986) and Tapponier *et al.* (1982) for eastern Asia, and Ratschbacher *et al.* (1989) and Vauchez & Nicolas (1991) for the Alps. Tectonic escape or 'lateral extrusion', was first suggested for southern China by Molnar & Tapponier (1975). It is considered today to be a lithospheric process and not limited to the crust (Vauchez *et al.* 1998) and is sometimes, but not always, accompanied by the extensional collapse of the thickened crust that is acted on by the compressive indenter. The indenter expels the thickened crust toward a weakly constrained lateral boundary. In this paper we will specifically extend the concept of crustal escape to the uppermost mantle in order to explain the observed mountain-parallel *Pn* anisotropy. In addition, we consider tectonic escape as being intimately connected with strong creep processes. These processes will be strongly enhanced by a preferred orientation of olivine crystals that produces a 'streamline-orientated' anisotropic viscosity which may assume a difference of the order of 10–100 between 'shear' and 'normal' viscosity (Christensen 1987).

MECHANISMS OF CREATING ANISOTROPY AT VARIOUS LEVELS IN THE LITHOSPHERE

So far, no regionally continuous seismic anisotropy has been observed in the *upper crust*, but we here describe its properties as a

juxtaposition to the other levels of the lithosphere. Anisotropy in the upper crust (∼10–15 km depth) is often caused by open, fluid-filled cracks that are created in the brittle crust (Kern 1982, Table 1). Aligned cracks may produce 'extensive dilatancy anisotropy' (EDA) that is significant at low confining pressures (Crampin 1984, 1989). At pressures greater than 200–300 MPa much of this anisotropy disappears owing to the closure of the cracks (Kern 1982). Evidence for connected cracks and large-scale, multiple fractures is given by prominent seismic reflections recorded from the brittle upper crust (Rabbel 1994; Meissner 1996). Only if the cracks are filled by melt might the anisotropy increase (Mainprice & Nicolas 1989).

Most rocks in the *upper crust* were formed at greater depth where temperatures and pressures produced anisotropy owing to foliation and mineral orientation (Brocher & Christensen 1990). Many of these rocks preserve their 'frozen-in' or 'fossil' anisotropy when transported to the upper crust. This is observed, for example, in the gneissic rocks of the deep continental drilling borehole (KTB) in southern Germany (Rabbel 1994; Rabbel & Mooney 1996) and some other locations (Mainprice & Nicolas 1989). Mylonitic and ultramylonitic rocks with strong mineral orientation are also common in the upper crust. Examples are found in association with the Ivrea Body in the Alps (Siegesmund & Kern 1990), the Santa Rosa Mylonite Zone (Kern & Wenk 1990), the Urals (Kashubin *et al.* 1984), the Alaska Range (Mayrand *et al.* 1987), the Black Forrest, Germany (Lueschen 1994) and the Wind River Thrust, Wyoming, USA (Jones & Nur 1984). These examples show mainly a local anisotropy, depending on the specific tectonic process.

Seismic anisotropy is more difficult to quantify in the *middle* and *lower crust*. This portion of the crust shows a wide range of seismic velocities and seismic reflectivity patterns (Mooney & Meissner 1992). Estimates of temperatures at the base of the crust range from 350°C beneath Archean cratons (e.g. Artemieva 1998; Artemieva & Mooney 2001) to 900°C in the Basin and Range Province (Lachenbruch & Sass 1978). In regions of crustal extension, seismic reflection profiles show near-horizontal lamellae-type reflectivity that is usually confined to the lower crust (Meissner 1989). This reflectivity appears to be caused by layering of elongated bodies with contrasting impedance, that almost certainly occurs by shear processes in a high-temperature, low-viscosity environment. These processes will certainly align anisotropic minerals (such as biotite and hornblende), and the ongoing strain is an ideal condition for creating lower crustal anisotropy (Mainprice & Nicolas 1989). However, in general lower crust anisotropy has so far been poorly investigated. An exception is the Urach region of southern Germany (Rabbel *et al.* 1998; Weiss *et al.* 1999), a small geothermal anomaly. Considering that the last regional tectonic event for most of Western Europe was the collapse of the Variscan mountain ranges, lower crust anisotropy of the LPO type is probably a regional feature. Lower crust anisotropy has not been quantified in cratonic environments.

In the *uppermost mantle* the dominating type of rock is peridotite, and olivine is inferred to contribute 60–75 per cent to its composition (Anderson 1989; Ismail & Mainprize 1998). The LPO of olivine plays the dominant role in determining seismic anisotropy (Peselnik *et al.* 1977; Ekström & Dziewonski 1998; Smith & Ekström 1999), while pyroxenes and other minerals seem to have a negative influence on the seismic anisotropy (Nicolas & Christensen 1987). There is convincing experimental evidence (Chastel *et al.* 1993; Tommasi *et al.* 1999) and seismological reasoning (Savage 1999) that the olivine *a*-axis aligns parallel to, or within 30° of, the direction of shear (Nicolas & Poirier 1976; Nicolas & Christensen 1987). Regions deformed at temperatures above 900°C and then cooled below 900°C may be considered to have their anisotropy 'frozen-in' (Silver & Chan 1991). This applies, for example, to the cratonic mantle and the 'mantle lid' below the Moho in non-cratonic regions (Anderson 1989). Frozen-in (or 'fossil') anisotropy may be modified by later tectonic or thermal events (Vauchez *et al.* 1997, 1998). Recrystallization plays a major role at large strains (Wenk & Tomé 1999). In general, the anisotropy we observe today is a manifestation of ductile deformation, dynamic recrystallization and annealing. Hence we cannot expect that the original anisotropy will be completely preserved.

OBSERVATION OF AZIMUTHAL ANISOTROPY IN THE UPPERMOST MANTLE

There are abundant observations on azimuthal mantle anisotropy, and most investigators use *SKS* waves to measure shear-wave splitting or relative residuals of *P* waves approaching seismological stations from different directions (Babuska & Cara 1991; Vinnik *et al.* 1992). These authors relate their observations to either frozen-in or young lithospheric anisotropy (Silver & Chan 1991; Silver 1996), or to asthenospheric anisotropy owing to deformation associated with plate motion (Vinnik *et al.* 1992). There have also been attempts to calibrate seismic observations with deformation observed in mantle xenolith samples (Ji *et al.* 1994; Bormann *et al.* 1996). Nevertheless, the depth extent and distribution of anisotropic rocks remain an open question, and some *SKS* studies have supported multiple layers of anisotropy. It is generally agreed that azimuthal anisotropy is globally present to a depth of about 200 km, and some of the observed anisotropy, especially in cratonic areas, is probably frozen-in (Drummond 1985; Ekström & Dziewonski 1998). However, anisotropy must also be present within the asthenosphere since regions with thin lithosphere, such as the Basin & Range Province and the eastern Snake River Plain in the western USA, also show strong shear wave splitting. For our studies of creep in the shallow mantle below young orogens we mainly rely on the *Pn* observations of Smith & Ekström (1999).

As mentioned before, *Pn*-wave studies of seismic anisotropy generally are limited to the upper 50–100 km of the mantle. As an example, refraction profiles of 300–500 km length sample the uppermost mantle down to a depth of 70–90 km (Walter & Flueh 1993; EUROBRIDGE Working Group 1999). However, at these depths *Pn* velocities (and traveltimes) are not always continuous. It seems, however, that low-frequency teleseismic waves are nearly continuous up to 1000 km offset (Smith & Ekström 1999).

MOUNTAIN-PARALLEL CREEP IN THE LOWER CRUST AND THE UPPERMOST MANTLE

Based on a large body of seismological data the generation of *Pn* anisotropy with the fast direction parallel to the structural axis of young mountain belts has been attributed to creep in the uppermost mantle (Smith & Ekström 1999). However, so far, no rheological or tectonic arguments were provided. In the following we use the term creep (instead of flow) to describe the slow solid-state processes of crystal alignment that causes the orientation of olivine crystals. Their fast axes (*a*-axes) will orientate themseves parallel to the creep direction, as was already suggested by Nicolas & Poirier (1976) Durham & Goetze (1977) and Babuska (1981). (See also Vinnik *et al.* 1992; Ji *et al.* 1994; Smith & Ekström 1999).

Assuming a typical continental geotherm (Chapman 1986) and creep parameters (Kirby & Kronenberg 1987) we solve Weertman's

equation (Weertman 1970) for the lithospheric viscosity, η (Meissner & Mooney 1998):

$$\ln \eta = (1/n)[(E_o/RT) + (1-n)\ln \dot{\varepsilon} - \ln C_n] \quad (2)$$

where n is the exponent (ranging from 1 to 4), in the following $n = 3$ is used; E_o is the creep activation energy, R is the gas constant; T is the absolute temperature; $\dot{\varepsilon}$ is the creep rate; C_n is a constant, depending on n, $\log C_n$ is about 13–17 GPa^{-n} s^{-1}.

Rutter & Brodie (1991), Meissner & Mooney (1998) and Porth (2000) discuss the validity and applicability of this equation. The wide range of possible activation energies determined in high P–T experiments for dry or wet olivine mantle provides a wide range of viscosity. In addition, the estimate of the creep rate at various levels makes any calculation of absolute viscosity very uncertain. As an additional factor, Kohlstedt & Zimmerman (1996) summarize evidence for substantial rheological weakening caused by a small amount of melt. These variables lend uncertainty to calculated viscosity–depth models. The most reliable conclusions regarding lithospheric viscosity are the viscosity jump at the Moho, caused by a large increase in activation energies, and the correlation between the thickness of the brittle part of the crust and the depth distribution of earthquakes (Sibson 1982; Meissner & Strehlau 1982; Lamongtange & Ranalli 1996). We strongly believe that the laboratory experiments of Mackwell *et al.* (1985, 1998) on dry diabase do not reflect the true composition of the lower crust in warm areas. Recently, Ranalli (2000), presented several rheologically different models, all of them showing an increase of viscosity at the crust mantle boundary.

For isotropic rocks there is an empirical relationship between seismic velocity and activation energy, and hence between velocity and viscosity (Meissner *et al.* 1991). For anisotropic rocks the situation is more complicated. There is petrological evidence that the (fast) a-axis of olivine crystals will cluster around the preferred creep direction (Nolet & Wortel 1989). Low strain and a recrystallization at large strains cause deviations and scatter (Wenk & Tomé 1999). Many researchers, (e.g. Karato & Wu 1993; Kohlstedt & Zimmerman 1996; Wendt *et al.* 1998) report that the preferred orientation of olivine is developed by dislocation creep. Vauchez *et al.* (1997) suggest that the existence of a pervasive fabric in the mantle induces anisotropic strength and viscosity. The maximum viscosity ratio for single olivine crystals could easily reach a factor of 10 (Vauchez *et al.* 1998). Even a factor of 10–100 is considered for a rock aggregate under favourable conditions (Christensen 1987). A factor of 10 has been used for the curves in Figs 1(a) and (b), showing the difference of anisotropy of viscosity. It is compatible with the seismic anisotropy, as seen at an ultramafic section of ophiolites, which show a 6–8 per cent anisotropy originating from preferred orientation of olivine (Christensen 1987), or a seismologically determined *Pn* anisotropy up to 10 per cent in some continental structures (Babuska & Cara 1991; Smith & Ekström 1999). Because of the suggested anisotropy of viscosity we believe that creep along low-viscosity streamlines might also provide a certain stabilising effect by a feedback mechanism.

We assume Weertman's power-law creep is valid for the lower crust and the upper mantle to the Lehmann discontinuity at a depth of 160–220 km and a temperature of 1200–1300°C. This accords with arguments for the dislocation creep above and diffusion creep below the Lehmann discontinuity (Karato & Wu 1993; Gaherty & Jordan 1995; Ribe 1989). Thus, we adopt the model of the Lehmann discontinuity as the boundary between an anisotropic uppermost mantle above and an isotropic mantle below. However, other models

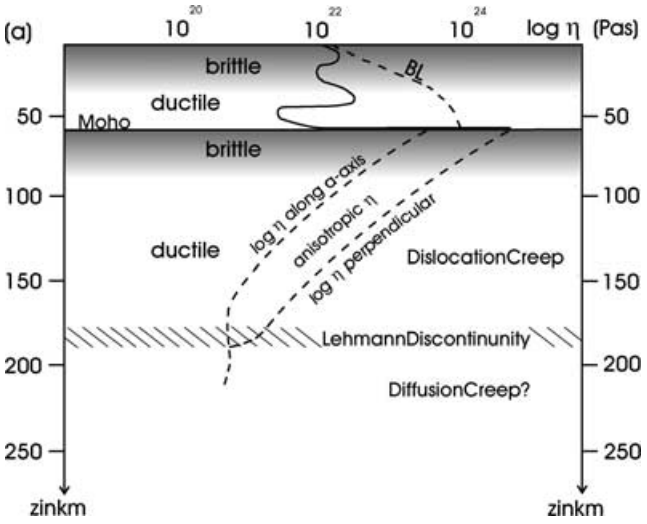

Figure 1a. Rheology and its anisotropy in (warm, thick) crust and upper mantle of young mountain belts; surface heat flow $q_0 = 70$ mW m^{-2}. BL = Byerlee's Law (extrapolated), strain rate $\dot{\epsilon} = 10^{-14}$ s^{-1}; other parameters from Kirby & Kronenberg (1987), anisotropy of viscosity (η) from various experimental studies (see text) of olivine (for the mantle) and other anisotropic minerals (crust). Please note that the assumption of a slower creep rate results in higher viscosity values (e.g. η is two orders of magnitude higher for a creep rate of 10^{-17} s^{-1} instead 10^{-14} s^{-1}). The right-hand η-curve in the diagram has been calculated according to Weertman's formula, the left-hand curve has been estimated to result in one order of magnitude lower viscosities along the olivin a-axes (see text).

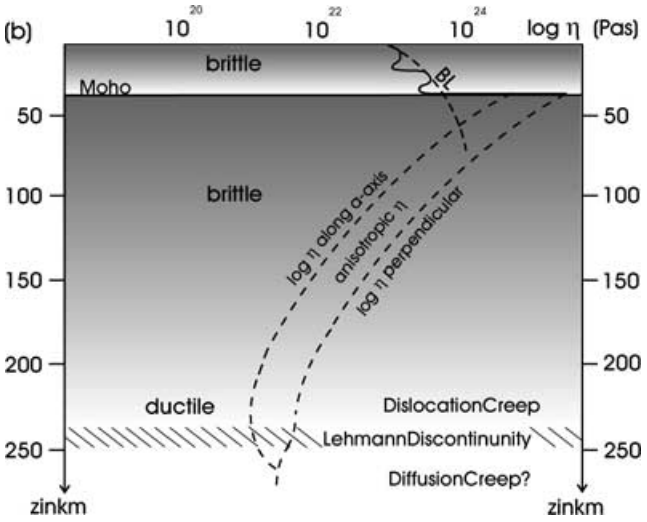

Figure 1b. Rheology and its anisotropy in the lithosphere of an ancient shield area, surface heat flow $q_0 = 40$ mW m^{-1}; other symbols and parameters as in Fig. 1(a).

do exist (Leven *et al.* 1981; Anderson 1989; Vinnik *et al.* 1992) postulate a strong contribution to anisotropy from the asthenosphere.

Two rather extreme rheological models are presented based on Byerlee's law (Byerlee 1978) and Weertman's equation (Weertman 1970) (eq. 2, Figs 1a and b). For the cratonic model (Fig. 1b), the whole crust is rigid (or has only a very small possible zone of weakness at the bottom), and also the upper mantle down to nearly 250 km depth. In contrast, the model for young orogens (Fig. 1a) shows extensive zones of weakness in the lower crust and in the upper mantle that may have only a thin rigid lid beneath the Moho. Young

mountain belts have a thick crust, higher-than-average heat flow, and higher upper mantle temperatures (Artemieva & Mooney 2001), which is possibly a consequence of additional heat from friction or some melt associated with deformation (Chapman 1986; Silver 1996). Hence, the orogenic lithosphere is weak, favouring creep with associated anisotropy in the lower crust and the uppermost mantle. In contrast, a weak layer in the mantle is expected beneath old cratons at much greater depth (below ∼70 km), in accordance with studies of the Canadian Shield where an anisotropic layer was found at a depth of 75–85 km (Bostok 1997).

Mountain-parallel creep in the uppermost mantle must be somehow connected to the tectonic forces acting perpendicular to the axis of the orogen (Vauchez & Nicolas 1991). The brittle upper crust and thin mantle lid respond to these compressional forces elastically, whereas the middle/lower crust and submantle-lid respond visco-elastically or ductilly (Fig. 2a). This compression will contribute to crustal uplift and, under appropriate conditions, lateral escape of middle and lower crustal material (and presumably weak mantle material) in the direction of the weakest part of the belt. Tectonic escape is directed to the east/southeast in Tibet, to the west in Turkey, and to the east in the Alps (Meissner & Mooney 1998). A major complication in the simple model of Fig. 2(a) comes from the structure of the compressed lithosphere. During the shortening process a cold, rigid indentor, a subduction or a delamination might occur, such as in the Alps (Heitzmann *et al.* 1991; Stampfli *et al.* 1998). This will definitely cause some movement of rigid and ductile material along the indentor, probably with a significant dip and mountain perpendicular component. Such a dipping component of the fast axes of anisotropy has been found in some older mountain belts by seismological traveltime delays of *Pn* (Babuska & Cara 1991). It seems to follow the direction of a fossil subduction zone. However, according to new studies from Smith & Ekström (1999) it is apparently not significant compared with the movement of lateral escape and the observed mountain-parallel LPO in young orogens.

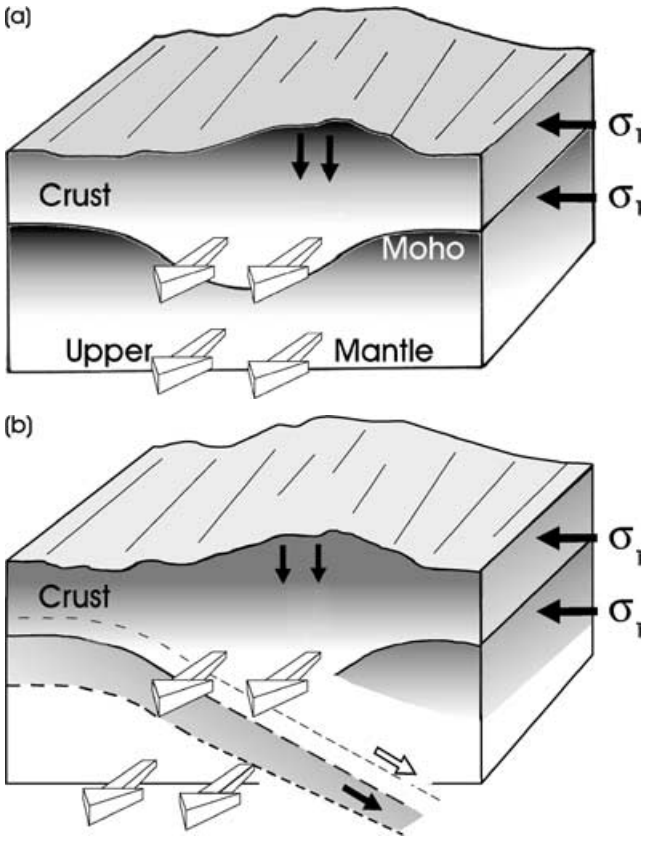

Figure 2. Conceptional model of a young mountain belt with mountain-perpendicular stresses σ_1 (black arrows). Mountain-parallel creep and possibly some escape take place in the ductile sections of lower crust and upper mantle, providing an explanation for the generation of mountain-parallel anisotropy (white arrows) Fig. 2(a): simple mountain range; Fig. 2(b): mountain range with an ongoing subduction or delamination.

The actual mechanism for creating mountain-parallel LPO in a mountain-perpendicular stress system is still hotly debated. Tommasi *et al.* (1999) give an explanation based on the experimental investigation of 200 naturally deformed olivine samples, using an anisotropic viscoplastic model. In order to explain the LPO directions they need pure or simple shear and a transpressional stress system. The observed mountain-parallel *S* wave polarization cannot be produced by a perpendicular subhorizontal deformation zone according to their model. They speculate that transpression in a vertical shear zone and/or a thick crust, decoupled from the mantle with a different stress system at depth, may play a role. A similar approach is applied by Wenk & Tomé (1999) who use visco-plastic polycrystal plasticity theory and even include recrystallization. They conclude that nucleation dominates recrystallization and observe an orientation of *a*-axes close to parallel in the shear direction. They speculate that the developement of preferred orientation is achieved 'during convection'.

Both groups of authors (Tommasi *et al.* 1999; Wenk & Tomé 1999) work with visco-plastic models. A completely different approach is the old expulsion calculation by Jaeger & Cook (1976) with completely ductile material beween approaching rigid boundaries. No ansiotropic minerals are involved and no anisotropy results from their numerical experiments. The lateral expulsion, however, might simulate our tectonic escape, the approaching boundaries might be our convergent compressive tectonics. And all modern researchers agree that LPO develops by the orientation of anisotropic minerals along the streamlines. The simple 2-D model for the expulsion of ductile material (direction x, velocity V_x) under approaching rigid boundaries (direction y, velocity V_y) gives

$$V_x = V_y \cdot x/a, \tag{3}$$

where a is the distance between the approaching boundaries.

A special 3-D model has been solved for a cylinder under radial compression (Hill 1965). We supply a more general solution in the Appendix. The important conclusion is that mountain-parallel creep under perpendicular stress is physically plausible. The estimated velocities are of the same order as the relative plate velocities, assuming an upper-mantle viscosity of 10^{21}–3×10^{22} Pa s.

There are two consequences of the extrusion model for the ductile middle and lower crust: (1) anisotropic minerals will align in the creep direction creating LPO and (2) the brittle upper crust is carried on top of the creeping lower crust during escape, forming characteristic fault patterns at the surface. The upper mantle below the thin mantle lid is considered to be ductile, too. As viscosity is especially low in the direction of creep (after the orientation of the *a*-axes of olivine) there will be a stabilization by the azimuthal differences of the viscosity (Fig. 1). Vauchez *et al.* (1997, 1998) uses the expression 'mechanical anisotropy' to explain the azimuthal dependence of strength and viscosity in orogenic belts and relates them to the preferred direction of later rift development that parallels the old orogenic direction.

OBSERVATIONS OF SEISMIC ANISOTROPY AND TECTONIC ESCAPE IN YOUNG OROGENS

As mentioned, young mountain belts exhibit mountain-parallel anisotropy that we attribute mainly to orientation of the olivine *a*-axes by creep (Silver 1996; Smith & Ekström 1999; Vauchez *et al.* 1997). We presume that the fast axes are subhorizontal, although deviations have been observed in older mountain belts and in some zones of collision (Babuska & Cara 1991). Young mountain belts with thick crust usually show indications of crustal escape, but it has been measured only in some cases, as discussed below.

Tibet

During the long period of convergence between India and Asia, the Tibetan Plateau has developed the highest elevation and the thickest crust (70–80 km) on Earth (Tapponier *et al.* 1982, 1986; Bird 1991; Li & Mooney 1998). The heat flow is higher than average, and seismic data have been interpreted to indicate either hydrothermal fluids or partial melting at a depth of 20 km in southern Tibet (Nelson *et al.* 1996; Makovski & Klemperer 1999). Many N–S-directed extensional faults and W–E-directed strike-slip faults indicate crustal escape (Molnar & Tapponier 1975; Zhao & Morgan 1987; England & Houseman 1989; Vauchez & Nicolas 1991). The cratonic Indian lithosphere intrudes the Plateau from the south and has reached at least the middle of the Plateau (Beghoul *et al.* 1993). *Pn* and *Sn* velocities are lower beneath the northern Plateau than in the south, and an asthenospheric upwelling has been suggested in the north. Following Zhao & Morgan (1987) the intruding Indian lithosphere created the thickening and warming of the Tibetan crust which responded as a viscous fluid in the middle and lower crust, hydraulically raising the plateau surface to a rather uniform level (Westaway 1995; Kola-Ojo & Meissner 2001).

According to Smith & Ekström (1999) no uniform azimuthal orientation of *Pn* is reported for Tibet. However, there are several shear wave splitting observations with a large azimuthal anisotropy along some profiles through southern and central Tibet (Hirn *et al.* 1998, 1995; Lavé *et al.* 1996; McNamara *et al.* 1997; Huang *et al.* 2000). In Fig. 3 we have plotted the more recent data of Huang *et al.* (2000) along the geophysical transect INDEPTH III. These data are based on more than 9 months recording time and are considered to be very reliable. The anisotropy data of McNamara *et al.* (1997) are added, while the older and often contradictory data have been omitted. The latest investigation (Huang *et al.* 2000) shows a substantial correlation of anisotropy with the strike of the Banggong–Nuijang Suture (BNS), suggesting some contribution from the crust and the (shallow) mantle. The BNS with its large strike-slip components has recently been shown to have a southerly dip in the upper 30 km (Meissner *et al.*, in preparation), and the advancing subcrustal Indian lithosphere is observed in receiver function displays further east (Kosarev *et al.* 1999).

All the new data are consistent with a model in which hot and weak upper mantle and lower crust are being squeezed eastward (strong azimuthal anisotropy) between the northward advancing and probably dipping subcrustal lithosphere (with weak azimuthal anisotropy) and the older northern lithosphere (Huang *et al.* 2000; Yuan *et al.* 1997). The available shear wave splitting data indicate that a

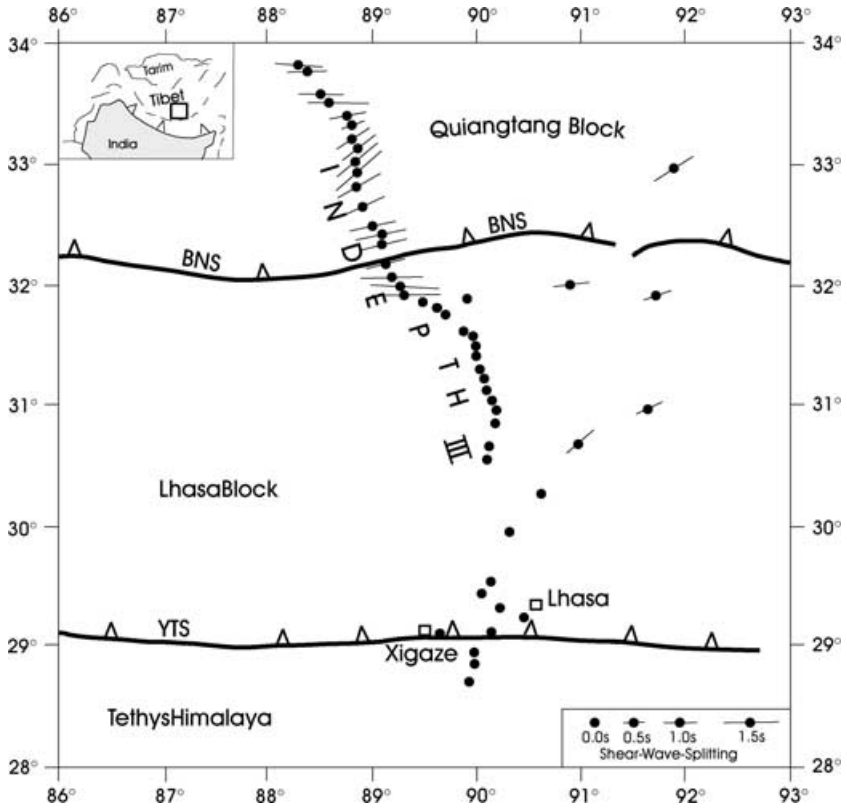

Figure 3. *SKS* anisotropy in southern Tibet; mainly from Huang *et al.* (2000) along profile INDEPTH III, and some older measurements. Note correlation with the (Jurassic) Banggong–Nuijang Suture (BNS). YTS = Yarlung Tsangpo Suture = latest suture in Tibet (Tertiary), dividing the Lhasa Block from the Tethyan Himalaya.

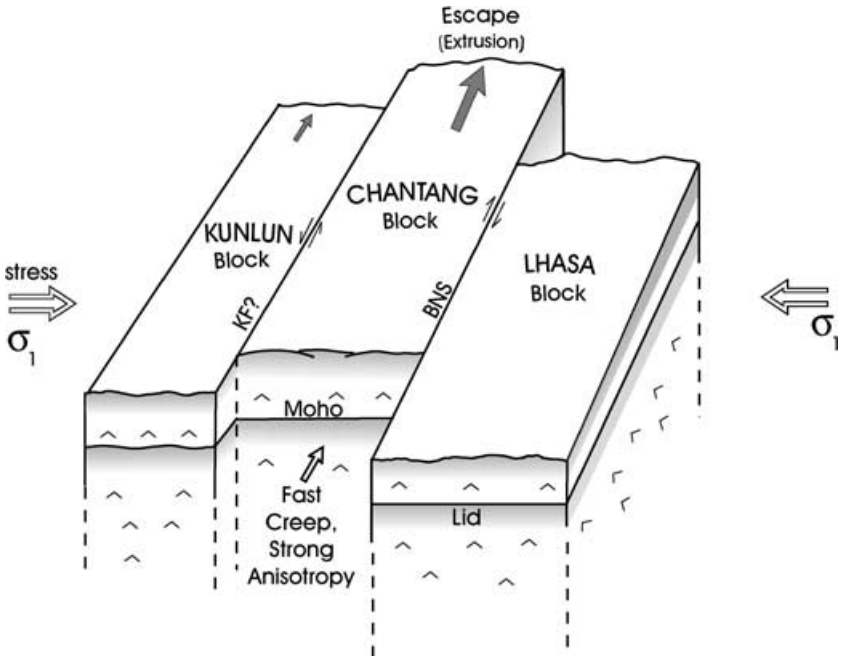

Figure 4. Conceptual model of the tectonic situation in Central Tibet with eastward extrusion of the Chantang (= Quiantang) Block; BNS = Bangong–Nuijang Suture; KF? = Kunlun Fault?

massive creep of mantle material is directed eastward in central Tibet. The correlation between the direction of anisotropy and surface structures suggests some contribution from the crust, although such a contribution seems to be small, as suggested by McNamara *et al.* (1997). Molnar & Tapponier (1975) introducing their slip line concept, later Vauchez & Nicolas (1991) and many others studying surface structures in Tibet suggest the presence of 'lateral extrusion', later termed 'tectonic escape'. Although reliable *P*-wave measurements are missing the strong and homogeneous shear wave data suggest that the whole lithosphere in central Tibet 'escapes' toward the weak lithospheric boundary in the east. Fig. 4 shows a conceptual extrusion model.

OROGENS NORTH OF THE MEDITERRANEAN SEA

From 80 Ma there is a general N–S approach of Africa and Eurasia increasing from west to east (Lliboutry 1999, p. 331). This movement was connected with the closing of the Tethys ocean and the northward movement of African promontaries, and was accompanied by high compressive stresses, complex rotation and the lateral escaping of terranes. Consequently, orogens with distinct structures were created from the Iberian Peninsula in the west to the Caucasus and Zagros mountains in the east. Mantle creep, resulting in seismic anisotropy, was certainly involved during the various tectonic phases. Smith & Ekström (1999) show two maps of *Pn* and *SKS* anisotropy for the Mediterranean area. These maps provide an estimate of the various depth levels of anisotropy. We have simplified the maps and added some information on stresses and lateral escape of terranes (Fig. 5).

In the east, the collision between Arabia and Asia started about 10 Ma (Burke & Sengör 1986). The rapid convergence has produced crustal thickening and an elevation of 3 km in the Zagros and Caucasus Mountains. Consequently, the portion of Turkey between the northern and southern Anatolian faults is escaping westward, as documented by fault geometry and focal mechanism solutions (Sengör *et al.* 1985). SE–NW-directed compressive stresses produce right-lateral slip along the northern Anatolian fault zone (NAFZ) at about 3 cm a^{-1}. The western escape of Turkey is directed toward the Aegean Sea, which is inferred to have a thin and weak lithosphere. While there is a strong mountain-parallel *Pn* anisotropy in the Caucasus, many experiments in western and central Turkey show that *Pn* anisotropy is surprisingly absent here (Smith & Ekström 1999). Sporadic *SKS* anisotropy show that the fast axis is directed SW–NE (Silver 1996), probably sampling deeper levels in the mantle. Although the lateral boundaries, especially the NAFZ, may consist of deep and even ductile strike-slip faults (Vauchez & Nicolas 1991), the absence of *Pn* anisotropy suggests that only the lower crust and not the whole lithosphere is participating in tectonic escape in Turkey. In the Caucasus the fast axes of *Pn* anisotropy are directed exactly along the mountain range while the *SKS* data show a slight deviation (Silver 1996).

The Alpine Chains, i.e. the Alps, Appenines, Pyrenees, Carpathians, Dinarides and Hellenides each have a unique tectonic history. The Alps began to develop in the Mesozoic, but their modern expression is caused by rapid Neogene convergence between the indenting Adriatic microplate and Europe (Nicolas *et al.* 1990; Heitzmann *et al.* 1991; Stampfli *et al.* 1998). Interwedging and interfingering into the European crust has caused a very complex tectonic structure with rheological layering that seems more or less to resemble the situation of our Fig. 2(b). Several nappes were thrust across the mountain range during the process of crustal shortening. The strongest compression is concentrated on the arc-like western Alps. The central and eastern Alps are laterally escaping eastward toward the thin and weak lithosphere of the Pannonian (Hungarian) Basin (Fig. 5). Evidence for tectonic escape is provided by faulting in the eastern Alps, by a sinistral strike-slip displacement

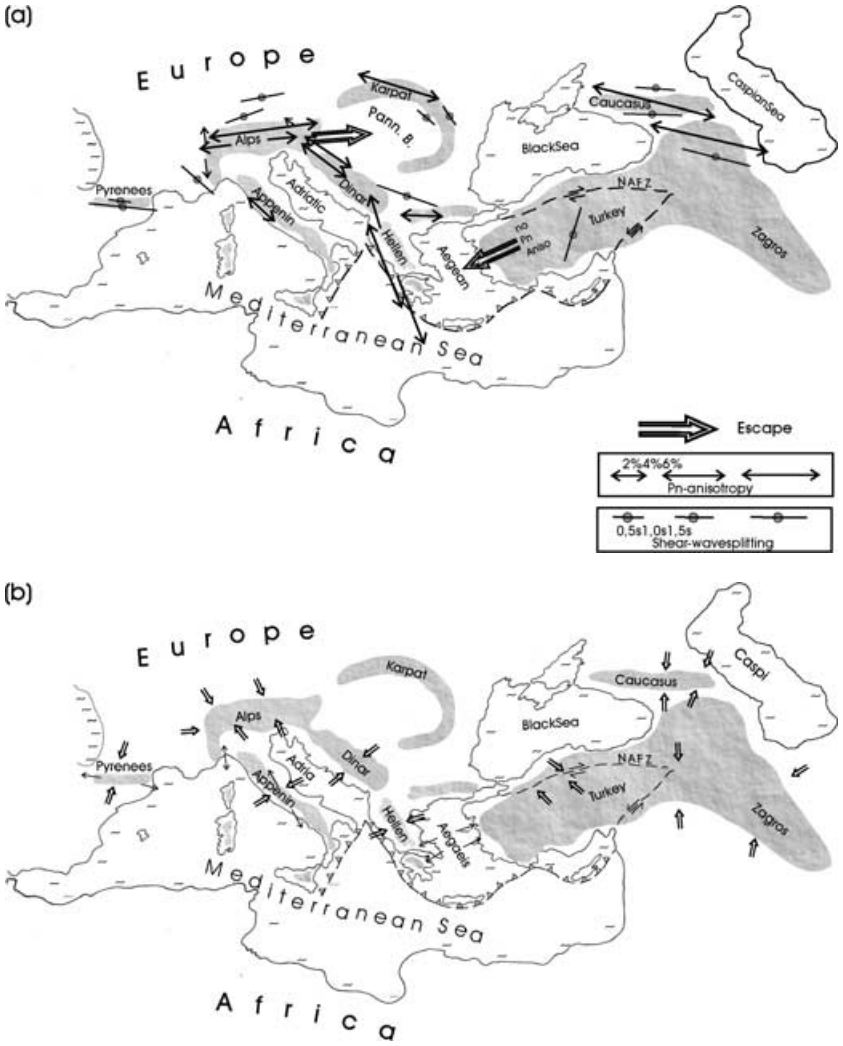

Figure 5. Comparison of fast P_n–axes, main compressive stresses and tectonic escape in young orogens north of the Mediteranean. Fig. 5(a) Fast axes of *Pn* and *SKS*. Length of arrows represent strength of anisotropy (from Silver 1996; Smith & Ekström 1999; Dricker *et al.* 1999). Note that central Turkey, although escaping to the W, shows zero *Pn* anisotropy in the upper mantle. Geologic boundaries, subduction in the eastern Mediteranean, and major fault zones in Turkey are indicated in the figure. Escape of Turkey and the Alps are marked by big arrows, simplified after Ratschbacher *et al.* (1989). Fig. 5(b) Main compressive stresses in young orogens; simplified after Zoback *et al.* (1989). Note deviation between the directions of stresses and fast anisotropy axes.

along the Insubric line, the surface expression of the southern limit of the European Alps (Lliboutry 2000), and also by large right-lateral strike-slip faults in the south (Ratschbacher *et al.* 1989). Both fast axes of *Pn* and *SKS* splitting maxima are observed to be mountain-parallel beneath the Alps (Smith & Ekström 1999; Silver 1996). Apparently, the fast axes of olivine are directed W–E, an observation that supports large-scale escape of the whole lithosphere to the east. The Alps provide some of the best evidence for tectonic escape of the lower crust and upper mantle beneath young orogens.

The Apennines of Italy are of Tertiary age, and formed in response to the westward subduction of lithosphere beneath the Corsica–Sardinia continental margin (Doglioni 1991). While several nappes progressed eastward, active normal faulting occurs within the western Apennines and indicates localized extension (Elter *et al.* 1975). The fast axis of *Pn* anisotropy is orientated parallel to the structural axis of this young orogen (Mele 1998), and *SKS* splitting measurements are within about 45° of this direction (Margheriti *et al.* 1996). Normal faulting within the western Apennines is consistent with tectonic escape of the middle and/or lower crust, although additional tectonic evidence is missing.

The formation of the Pyrenees is connected with the Cretacious rotation of the Iberian Peninsula of ∼30° anticlockwise, accompanied by the opening of the Bay of Biscay, and with the final docking of Iberia to Europe. Compared with the other Alpine chains the Pyrenees are surprisingly straight, possibly an indication of large amounts of strike-slip movement, and are very symmetric. To the north there is a pronounced E–W-directed transform fault (e.g. Schönenberg & Neugebauer 1987; Barruol *et al.* 1997). The ECORS near-vertical reflection survey (ECORS Pyrenees Team 1988) recorded a strong reflector interpreted as an indentor. The maximum Moho depth is nearly 60 km in the centre of the orogen with a possible northward subduction or delamination zone. There are no *Pn* recordings in the Pyrenees. However, very strong *SKS* splitting, with a maximum parallel to the mountain range has been observed by Barruol *et al.* (1997). This indicates large-scale creep of the lithosphere or even the asthenosphere along the mountain range.

There are two *SKS* studies and only one *Pn* observation in the Carpathians. The fast axes are mountain parallel, but a general statement is not justified in view of the highly varying strike of the mountain. While the structure of the Dinarides seems to be a kind of SE attachment to the eastern Alps, the Hellenides further south near the Ionian Sea seem to be a prolongation of the Dinarides. While Jurassic and Cretaceous processes laid the foundation of the mountains, compressional stresses in the Eocene and Miocene formed the main tectonic phases of the orogenies (Schönenberg & Neugebauer 1987). Hence, both mountain ranges, including the extension of the Hellenides into the Aegean, belong to the youngest orogenies in the Mediterranean area. Seismicity is high in both mountain ranges. Strong *Pn* anisotropy is seen in the northern Dinarides, and very strong and concentrated *Pn* anisotropy is oberserved in the Hellenides. The fast axes of anisotropy is strongly mountain parallel, indicating large-scale creep at least in the shallow mantle. *SKS* observations are missing.

In Figs 5(a) and (b) we compare the *Pn* anisotropy data of Smith & Ekström (1999) including the *SKS* data from Silver (1996) and Dricker *et al.* (1999) with selected stresses from Zoback *et al.* (1989) and Zoback (1992) for the young orogenies north of the Mediterranean. We see that in the whole area the mountain-parallel fast axes of anisotropy correspond closely to mountain-perpendicular tectonic stresses.

MOUNTAIN RANGES IN THE AMERICAS–ALASKA–ROCKY MOUNTAINS–ANDES

Alaska's mountain ranges belong to an active margin and are one of the youngest orogenies. Well-constrained *Pn* axes follow the curvature of the Alaskan range (Smith & Ekström 1999). *SKS* studies are slightly to the north of the range, but also follow the bending of the mountains (Wysession *et al.* 1996). Further south, along the Pacific coast the tectonic situation is more complicated and the fast directions of *Pn* and *SKS* rotate, sometimes even turning to a mountain perpendicular direction. However, in central and southern California *Pn* azimuths parallel the Sierra Nevada and confirm the results of early *Pn* studies of Vetter & Minster (1981). *SKS* studies in California, especially near the San Andreas Fault, indicate two different layers of anisotropy (Silver & Savage 1994), the upper layer showing similar anisotropy to the *Pn* studies. In the northern Rocky Mountains fast axes of *Pn* are nearly parallel to the mountain ranges while the fast axes from *SKS* studies are nearly perpendicular to them. It seems that again different layers in the lithosphere (or even asthenosphere) are involved. No clear indication for tectonic escape is seen.

The Andes are the result of a long-lived ocean–continent collision (Kearey & Vine 1990). Smith & Ekström (1999) report mountain-parallel *Pn* anisotropy in the southern Andes, and Silver (1996), Silver & Savage (1994), and Russo & Silver (1998) report mountain-parallel anisotropy of split *SKS* phases in the north and in the centre. The latter authors speculate concerning the existence of subhorizontal asthenospheric flow parallel to the strike of the subducting slab. However, observations from Japan show fast *Pn* axes, certainly sampling only the uppermost mantle, that are parallel to the strike of the subducting slab. This observation is also matched by *SKS* studies, indicating a large-scale island-parallel mantle creep. In the Central Andes, with crustal thickness of over 70 km in the Altiplano, partial melting is inferred for the middle crust extending north–south for more than 300 km based on numerous receiver function studies (Yuan *et al.* 2000). Hence, crustal escape is plausible but there is no reliable geologic information to confirm this suggestion. Kay *et al.* (1994) suggest an eastward lithospheric delamination, and this process may compete with lateral escape. A simplified summary of the *Pn* anisotropy of young mountain belts is listed in Table 2.

DISCUSSION

Estimates of temperature and viscosity below young (thick and warm) mountain ranges indicate that the physical conditions for ductile behaviour exists in at least two layers of the lithosphere: in the thickened ductile lower crust and in the uppermost mantle below a small rigid lid beneath the Moho (Fig. 1a). Orogenic stresses perpendicular to the axis of mountain ranges and the pressure of a thick crust provide the necessary strain for mountain-parallel creep and extrusion to be initiated. This is best established for *Pn* waves,

Table 2. Observation of azimuthal anisotropy in *Pn* and *SKS* and tectonic escape.

	Mountain parallel *Pn*	Mountain parallel *SKS*	Observed escape?	References
Tibet	Possibly	2.5 s	Yes	Be 93, Z 89, Mc 97, Yu 97
Caucasus	5%	1.5 s	No	Vi 92, Z 92, Si 96, SE 99
Turkey	No	No	Yes	Vi 92, Z 92, Si 96, SE 99
Alps	4%	1.2 s	Yes	Vi 92, Z 92, Si 96, SE 99
Appenin	3%	Unknown	Unknown	El 75, Me 98, Do 91, SE 99
Pyrenees	Unknown	2 s	Unknown	EC 89, Z 92, SE 99
Dinarides	3%	Unknown	Unknown	Vi 92, Z 92, SE 99
Hellenides	6%	Unknown	Possibly	Vi 92, Si 96, SE 99
Carpathians	5%	Unknown	Locally	Si 96, Dr 99, SE 99
Alaska	4%	1.5 s	Unknown	Wy 96, Si 96, SE 99
Sierra Nevada	4%	No	Unknown	VM 81, Z 92, SE 99, Wy 96
Rocky mountains	6% in the N	No	Unknown	Si 96, SE 99, Wy 96
Andes	6%	1.0 s	Unknown	Vi 92, Z 92, SE 99

Be 93 = Beghoul *et al.* (1993); Do = Doglioni (1991); Dr = Dricker *et al.* (1999); El 75 = Elter *et al.* (1975); EC 89 = ECORS Pyrenees Team (1988); Me 98 = Mele (1998); Z 89 = Zoback *et al.* (1989); Z 92 = Zoback (1992); Mc 97 = McNamara *et al.* (1997); Vi 92 = Vinnik *et al.* (1992); Si 96 = Silver (1996); SE 99 = Smith & Ekström (1999); VM = Vetter & Minster (1981); Yu 97 = Yuan *et al.* (1997).

sampling anisotropy in the uppermost mantle, but also *SKS* waves show very often (but not always) a mountain-parallel anisotropy. Lateral creep is directed toward a weaker area. We infer that it stabilizes with time because of the minimum viscosity of dominating minerals along certain structural axes: for the upper mantle creep these are the *a*-axes of olivines and for lower crustal creep there are the preferred axes for biotite and hornblende. Both weak areas develop LPO after the beginning of creep.

There are other explanations for mountain-parallel *SKS* anisotropy. Tommasi *et al.* (1999) and Vauchez & Nicolas (1991) suggested that oblique stresses along deep, lithospheric faults, rooted in the upper mantle, can support the horizontal extrusion of large parts of the lithosphere, generating a horizontally directed LPO. On the other hand, the existence of deep lithospheric faults is certainly not supported by seismicity observation and seems doubtful based on rheological estimates in warm areas (Meissner 1989, 1996). Nevertheless, localized zones of enhanced shear and creep might exist and limit the extrusion of blocks and its anisotropy (Fig. 4). As mentioned above, there is no depth control for *S*-wave splitting.

Our concept for the creation of LPO anisotropy by ductile extrusion can explain the observations that the anisotropic fast axes are mountain-parallel below nearly all young mountain ranges (Smith & Ekström 1999). Based on *Pn* observations it is probable (but not certain) that the strongest development of creep and LPO anisotropy occurs in the shallow mantle, extending down to the Lehmann Discontinuity at a depth of 170–200 km (Karato & Wu 1993). This is because here dislocation creep is dominant, and this creep is known to cause LPO anisotropy (Nicolas & Christensen 1987; Wendt *et al.* 1998). To study the upper part of this shallow mantle depth the sampling of relatively short *Pn* branches is the most reliable method (Smith & Ekström 1999).

A surprising observation is the different depth level of the tectonic stress acting on the brittle upper crust on one hand and the response of the ductile layers (lower crust, upper mantle) on the other hand. The upper mantle and upper crust are decoupled by the ductile lower crust in warm areas. This is in contrast to the situation in old and cold cratonic areas, which are rigid throughout (Fig. 1b). Cratons may also be anisotropic, and we agree with previous suggestions that the *Pn* anisotropy found in cratons dates to their creation in the Precambrian (when these areas were young and warm) and is frozen-in (Silver & Chan 1991; Silver 1996). The existence of a rigid lithosphere with strong coupling in cratonic areas is supported by the observed correlation between the direction of anisotropy from *SKS*-type waves (which measure deep lithosphere or astenosphere) with the direction of plate motion, supposed to be guided by asthenospheric convection (Vinnik *et al.* 1992). In old orogens such as the Early Proterozoic Trans-Hudson Orogen, Canada the observed (*SKS*) anisotropy (Savage 1999) seems to be connected with plate motions or asthenospheric motions as the depth to the anisotropic layer exceeds the lithospheric thickness, estimated to be about 200 km for Proterozoic or older units (Artemieva & Mooney 2001).

Mountain-parallel *Pn* anisotropy (and probably mantle creep) is also found in young island arcs (Smith & Ekström 1999) inspite of down-going slabs that suggest at least some creep around and parallel to the subducted slab. Only Island-parallel creep like the mountain-parallel creep seems to determine the observed anisotropy, even in the presence of subducting slabs (Fig. 2b). We also studied the problem of tectonic escape and conclude that the uppermost mantle also may participate in lateral 'escape' from an active orogen. So far clear observations of escape, based on fault patterns, strike-slip movements and geodesy, are reported only for Tibet, Turkey and the Alps. In these three regions two conditions may play a role: (1) mountain ranges must be high and (2) tectonically weak zones must exist in the region adjacent to the axis of the mountain range. For Tibet the correlation of a prominent surface fault, the Banggong–Nuijang Suture, with the beginning of a broad zone of strong (*SKS*) anisotropy strongly supports the existence of an involvement of the whole lithosphere, including the crust (Fig. 4). The east–west directed strike-slip faults in central and northern Tibet might extend to great depth (Vauchez & Nicolas 1991). The advancing Indian subcrustal lithosphere and its very limited progress to the north, much less than the convergence rate of India would predict, provides another problem (Beghoul *et al.* 1993; Kosarev *et al.* 1999). The discrepancy between the predicted and the observed subcrustal lithopshere could be solved by assuming that the whole lithosphere is laterally (not only vertically) detached in a very widespread escape (Kola-Ojo & Meissner 2001). For Turkey the absence of any *Pn* anisotropy (and only one *SKS* observation) supports the assumption that not the subcrustal lithosphere, but possibly only the ductile lower crust is escaping. Its lateral limits might be the North- and the East-Anatolian faults that might become ductile at depth, but this cannot explain the fact that *Pn* anisotropy is completely missing. For the Alps *Pn* and *SKS* observations suggest that the whole lithosphere is involved in an eastward escape. The east–west running Insubric Line showing left-lateral strike-slip movement may act as a northern boundary of tectonic escape of the southern and eastern Alps escaping toward the hot and weak Pannonian Basin (Ratschbacher *et al.* 1989).

All three regions of tectonic escape are slightly different and ductile layers may have different thicknesses and depths. Nevertheless, we think that all three regions are comparable with a toothpaste tube model: compressive stress causes the most ductile interior to creep in a tube-parallel mode to an open exit. Certainly, this simple model does not involve any dislocation creep, orientation of anisotropic minerals or recrytallization. It only offers an explanation for the initiation of creep.

CONCLUSIONS

We have selected observations on seismic anisotropy in the continental crust and uppermost mantle and specifically in young mountain belts. We argue that they provide important evidence for deformation processes in the crust and the subcrustal lithosphere.

(1) Seismic anisotropy in the brittle upper crust is related to several factors, including orientated cracks, alignment of foliation in metamorphic rocks, and fine-scale lithologic layering. Cracks are closed in the middle and lower crust, and anisotropy there is due to the presence of anisotropic minerals (such as biotite and hornblende) that are aligned within a warm, low-viscosity environment. Seismic anisotropy in the upper mantle is well established worldwide and inferred to be produced by dislocation creep and LPO of anisotropic minerals, primarily olivine.

(2) Lithospheric rheology plays a dominant role in the creation and preservation of anisotropy in all levels of the lithosphere, thus we examine the viscosity–depth structure for two types of continental lithosphere. We find that there are two layers within the warm continental lithosphere that provide favourable conditions for creep and hence for producing anisotropy. The first favourable layer occurs within the lower crust and the second one begins below the mantle lid, i.e. at a depth of 10–30 km below the Moho. The depth and thickness of these layers depends on the geothermal gradient,

on the crustal and lithospheric thickness, and the composition of the crust and subcrustal lithosphere.

(3) The process responsible for formation of anisotropic layers in the continental lithosphere can be inferred from an examination of young orogens. Seismic data (mostly *Pn* refraction data; Smith & Ekström 1999) show that anisotropy in the shallow mantle is usually parallel to the structural axis of mountain belts (i.e. mountain-parallel), while compressional tectonic stresses, determined in the upper crust by focal plane solutions and drilling (Zoback 1992), show strong mountain-perpendicular components. The weak lower crust acts as a decoupling unit. Our viscosity models show that also the viscosity is anisotropic with the lowest viscosity along the fast axes of olivine orientated along the streamlines. The anisotropy of viscosity is compatible with the seismic anisotropy. It initiates an alignment of the anisotropic minerals and provides a feedback mechanism for stabilizing creep and seismic anisotropy along the fast mineral axes.

(4) We summarize observations of seismic anisotropy and upper crustal stress directions for Tibet, for the young mountains north of the Mediterranean Sea, and for young mountain belts in the Americas. Based on the strong azimuthal discrepancy between the mantle anisotropy and the crustal stresses, we postulate, in agreement with earlier suggestions (Vauchez & Nicolas 1991), that mountain-parallel creep occurs in the uppermost mantle beneath young orogens. Creep might become more pronounced and evolve into tectonic escape under special conditions, such as the existence of a weak tectonic unit near to the axis of the orogen. We extend the concept of tectonic escape (Burke & Sengör 1986) to the whole lithosphere. The weak layers in the lower crust and the upper mantle provide the condition for pronounced creep under stress. The compression of a horizontal, open toothpaste tube is a simple physical analogue for the initiation of creep and tectonic escape.

ACKNOWLEDGMENTS

Thanks are due to our colleagues from the USGS in Menlo Park and the Institute of Geoscience in Kiel who have helped to improve the original version of the manuscript, especially Bob Mereu, James Savage, Wolfgang Rabbel, Hartmut Kern, Ron Girdler and Shane Dettweiler. Special thanks go to Alain Vauchez and an anonymous reviewer for their critical and helpful comments.

REFERENCES

Anderson, D.L., 1989. *Theory of the Earth,* pp. 1–366, Blackwell, Boston, MA.

Artemieva, I.M., 1998. Subcrustal temperatures in Precambrian cratons: a comparative study, *Geophys. Monogr. ser.,* **20,** 626–675.

Artemieva, I.M. & Mooney, W.D., 2001. Thermal thickness and evolution of Precambrian lithosphere: a global study, *J. geophys. Res.,* **106(B8),** 16 387–16 414.

Babuska, V., 1981. Anisotropy of V_P and V_S in rock-forming minerals, *J. Geophys.,* **50,** 1–6.

Babuska, V. & Cara, M., 1991. *Seismic Anisotropy in the Earth,* pp. 1–207, Kluwer, Dordrecht.

Backus, G.E., 1962. Long wavelength elastic anisotropy produced by horizontal layering, *J. geophys. Res.,* **67,** 4427–4440.

Bamford, D., 1977. *Pn* velocity anisotropy in a continental upper mantle, *Geophys. J. R. astr. Soc.,* **49,** 29–48.

Barruol, G., Silver, P.G. & Vauchez, A., 1997. Anisotropy beneath the Pyrenees range from teleseismic shear wave splitting: results from a test experiment, *Geophys. Res. Lett.,* **16,** 493–496.

Beghoul, N., Barazangi, M. & Isacks, B.L., 1993. Lithospheric structure of Tibet and Western North America: mechanism of uplift and a comparative study, *J. geophys. Res.,* **98,** 1997–2016.

Bird, P., 1991. Lateral extrusion of lower crust from under high topography, in the isostatic limit, *J. geophys. Res.,* **96,** 10 275–10 286.

Bormann, P., Gruntha, G., Kind, R. & Montag, H., 1996. Upper mantle anisotropy beneath central Europe from *SKS* wave splitting, *J. Geodyn.,* **22,** 5–8.

Bostok, M.G., 1997. Anisotropic upper mantle stratigraphy and architecture of the Slave Craton, *Nature,* **390,** 392–395.

Brocher, T.M. & Christensen, N.I., 1990. Seismic anisotropy due to preferred mineral orientation observed in shallow crustal rocks in southern Alaska, *Geology,* **18,** 737–740.

Budsansky, B. & O'Connel, R., 1976. Elastic moduli at cracked solid, *Int. J. Solids Struct.,* **12,** 81–97.

Burke, K. & Sengör, C., 1986. Tectonic escape in the evolution of the continental crust, in *Reflection Seismology: the Continental Crust, AGU Geodynamic Ser.,* Vol. 14, pp. 41–53, eds Barazangi, M. & Brown, L. AGU, Washington.

Byerlee, J.D., 1978. Friction of rocks, *Pure appl. Geophys.,* **116,** 615–626.

Chapman, D.S., 1986. Thermal gradients in the continental crust, in *The Nature of the Lower Continental Crust, Geol. Soc. London, Spec. Publ.,* Vol. 24, eds Dawson *et al.* Geol. Society, London.

Chastel, Y.B., Dawson, P.R., Wenk, H.-R. & Bennet, K., 1993. Anisotropic convection with implication for the upper mantle, *J. geophys. Res.,* **98,** 17 757–17 771.

Christensen, U.R., 1987. Some geodynamical consequences of anisotropic viscosity, *Geophys. J. R. astr. Soc.,* **91,** 711–736.

Crampin, S., 1984. Effective anisotropic elastic constants for wave propagation through cracked solids, *Geophys. J. R. astr. Soc.,* **76,** 135–145.

Crampin, S., 1989. Suggestion for a consistent terminology for seismic anisotropy, *Geophys. Prospect.,* **31,** 753–770.

DeMets, C.R., Gordon, G., Argus, D.F. & Stein, S., 1994. Effect of recent revisions to the geomagnetic reversal time scale on estimate of curremt plate motion, *Geophys. Res. Lett.,* **21,** 2191–2194.

Doglioni, C., 1991. A proposal for kinematic modelling of W-dipping subduction—possible application to the Tyrrhenian–Apennines system, *TerraNova,* **3,** 423–434.

Dricker, I., Vinnik, L., Roecker, S. & Makeyeva, L., 1999. Upper mantle flow in eastern Europe, *Geophys. Res. Lett.,* **26,** 1219–1222.

Drummond, B.J., 1985. Seismic *P*-wave anisotropy in the subcrustal lithosphere of north-west Australia, *Geophys. J. R. astr. Soc.,* **81,** 497–519.

Durham, W.B. & Goetze, G., 1977. Plastic flow of oriented single crystals of olivine; 1. mechanical data, *J. geophys. Res.,* **82,** 5737–5753.

ECORS Pyrenees Team, 1988. The ECORS deep reflection seismis survey across the Pyrenees, *Nature,* **331,** 508–511.

Ekström, G. & Dziewonski, A.M., 1998. The unique anisotropy of the Pacific upper mantle, *Nature,* **394,** 168–172.

Elter, P., Goglia, G., Tongiorgi, M. & Trevisan, L., 1975. Tensional and compressional areas in the recent (Tortonian to present) evolution of the Northern Apennines, *Boll. Geofis. Teor. Appl.,* **27,** 3–18.

England, P. & Houseman, G., 1989. Extension during continental convergence, with application to the Tibet Plateau, *J. geophys. Res.,* **94,** 17 561–17 579.

EUROBRIDGE Seismic Working Group, 1999. Seismic velocity structure across the Fennoscandia–Sarmatia suture of the East European Craton, *Tectonophysics,* **314,** 193–217.

Fowler, M., 1990. *The Solid Earth, An Introduction to Global Geophysics,* p. 472, Cambridge University Press, Cambridge.

Gaherty, J. & Jordan, T.H., 1995. The Lehmann Discontinuity as the base of an anisotropic layer beneath continents, *Science,* **268,** 1468–1471.

Heitzmann, P., Frei, W., Lehner, P. & Valasek, P., 1991. Crustal indentation in the Alps—an overview; reflection seismic profiling in Switzerland; deep seismic reflections, *Geodynamics,* **22,** in *Am. Geophys. Union,* 161–176, eds Meissner, R. *et al.*

Helbig, K., 1984. Anisotropy and dispersion in periodically layered media, *Geophysics,* **49,** 364–373.

Hill, R., 1965. *The Mathematical Theory of Plasticity,*. 2nd edn, pp. 262–267, Clarendon Press, Oxford.

Hirn, A. *et al.*, 1995. Seismic anisotropy as an indicator of mantle flow beneath the Himalayas and Tibet, *Nature,* **375,** 571–574.

Hirn, A., Díaz, J., Sapin, M. & Veinante, J.L., 1998. Variations of shear-wave residuals and splitting parameters from array observations in southern Tibet, *Pure appl. Geophys.,* **151,** 407–431.

Huang, W.-C. *et al.*, 2000. Seismic polarization anisotropy beneath the central Tibetan plateau, *J. geophys. Res.,* **105,** 27 979–27 989.

Ismail, W.B. & Mainprize, D., 1998. An olivine fabric database: an overview of upper mantle fabrics and seismic anisotropy, *Tectonophysics,* **296,** 145–157.

Jaeger, J.C. & Cook, N.G.W., 1976. *Fundamentals of Rock Mechanics,* 2nd edn, pp. 1–585, Chapman and Hall, London/Wiley, New York.

Ji, S., Zhao, X. & Francis, D., 1994. Calibration of shear-wave splitting in the subcontinental upper mantle beneath active orogenic belts using ultramafic xenoliths from the Canadian Cordillera and Alaska, *Tectonophysics,* **239,** 1–27.

Jones, T.D. & Nur, A., 1984. The nature of seismic reflections from deep crustal fault zones, *J. geophys. Res.,* **89,** 3153–3171.

Karato, S. & Wu, P., 1993. Rheology of the upper mantle: a synthesis, *Science,* **260,** 771–777.

Kashubin, S.I., Pavlenkova, N.I. & Yegorkin, A.V., 1984. Crustal heterogeneity and velocity anisotropy from seismic studies in the USSR, *Geophys. J. R. astr. Soc.,* 1984, 221–226.

Kay, R.W., Coira, B. & Viramonte, J., 1994. Some mafic back arc volcanic rocks beneath the Argentine Puma Plateau, central Andes, *J. geophys. Res.,* **99,** 24 332–24 339.

Kern, H. & Richter, A., 1981. Temperature derivatives of compressional and shear wave velocities in crustal and mantle rocks at 5 kbar confining pressure, *J. Geophys.,* **49,** 47–56.

Kern, H., 1982. *P*- and *S*-wave velocities in crustal and mantle rocks under simultaneous action of high confining pressure and high temperature and the effect of the rock microstructure, in *High Pressure Researches in Geoscience,* pp. 15–45, ed. Schreyer, W., Schweizerbarth, Stuttgart.

Kern, H., Burlini, L. & Ashchepkov, I.V., 1996. Fabric-related anisotropy in upper mantle xenoliths: evidence from measurements and calculations, *Phys. Earth planet. Inter.,* **95,** 195–209.

Kern, H. & Wenk, H.R., 1990. Fabric-related velocity anisotropy and shear wave splitting in rocks from Santa Rosa mylonite zone, California, *J. geophys. Res.,* **95,** 11 231–11 223.

Kirby, S.H. & Kronenberg, A.K., 1987. Rheology of the lithosphere: selected topics, *Rev. Geophys, Space Phys.,* **25,** 1219–1244.

Kohlstedt, D.L. & Zimmerman, M.E., 996. Rheology of partially molten mantle rocks, *Ann. Rev. Earth planet. Sci.,* **24,** 41–62.

Kola-Ojo & Meissner, R., 2001. Southern Tibet: its deeo seismic structure and some tectonic implications, *J. Asian Earth Sci.,* **Febr.,** 249–256.

Kosarev, G., Kind, R., Sobolev, S.V., Yan, X., Hanka, W. & Orechin, S., 1999. Seismic evidence for a detached Indian lithospheric mantle beneath Tibet, *Science,* **283,** 1306–1309.

Lachenbruch, A.H. & Sass, J.H., 1978. Models of an extending lithosphere and heat flow in the Basin and Range province, in *Cenozoic Tectonics and Regional Geophysics of the Western Cordillera, Geological Soc. America Memoir.,* **152,** 209–250, eds Smith, R.B. & Eaton, G.P.

Lamongtange, M. & Ranalli, G., 1996. Thermal and rheological constraints on earthquake depth distribution in the Charlevoix intraplate seismic zone, *Tectonophysics,* **257,** 55–69.

Lavé, H.J., Avouac, J.P., Lacassin, R., Tapponier, P. & Montagner, J.P., 1996. Seismic anisotropy beneath Tibet: evidence for eastward extrusion of the Tibetan lithospere? *Earth planet. Sci. Lett.,* **140,** 83–96.

Leven, H.J., Jackson, I. & Ringwood, A.E., 1981. Upper mantle seismic anisotropy and lithospheric decoupling, *Nature,* **289,** 234–239.

Li, S.-L. & Mooney, W.D., 1998. Crustal structure of China from deep seismic sounding profiles, *Tectonophysics,* **288,** 105–113.

Love, A.E.H., 1927. A treatise on the mathematical theory of elasticity, p. 643, Dover, New York.

Lliboutry, L., 2000. *Quantitative Geophysics and Geology,* pp. 1–480, Springer, Berlin.

Lueschen, E., 1994. Crustal 'bright spots' and anisotropy from multicomponent *P*- and *S*-wave measurements in southern Germany, *Tectonophysics,* **232,** 343–354.

Mackwell, S.J., Kohlstedt, D.L. & Paterson, M.S., 1985. The role of water in the deformation of olivine single crystal, *J. geophys. Res.,* **90,** 11 319–11 333.

Mackwell, S.-J., Zimmerman, M.E. & Kohlstedt, D.L., 1998. High-temperature deformation of dry diabase with application to tectonic on Venus, *J. geophys. Res.,* **103,** 975–984.

Mainprice, D. & Nicolas, A., 1989. Development of a lattice preferred orientation of minerals, *Comput. Geosci.,* **16,** 385–393.

Margheriti, L., Nostro, C., Cocco, M. & Amato, A., 1996. Seismic anisotropy beneath the Northern Apennines (Italy) and its tectonic implications, *Geophys. Res. Lett.,* **23,** 2721–2724.

Makovski, Y. & Klemperer, S.L., 1999. Measuring the seismic properties of Tibetan bright spots: evidence for free aqueous fluids in the Tibetan middle crust, *J. geophys. Res.,* **104,** 10 795–10 825.

Mayrand, L.J., Green, A.G. & Milkereit, B., 1987. A quantitative approach to bedrock velocity resolution and precision, *J. geophys. Res.,* **92,** 4837–4845.

McNamara, D.E., Waller, T.R., Owens, T.J. & Ammon, C.J., 1997. upper mantle velocity structure in the Tibetan Plateau from *Pn*-traveltime anomaly, *J. geophys. Res.,* **102,** 493–505.

Meissner, R., 1989. Rupture, creep, lamellae & crocodiles: happenings in the continental crust, *TerraNova,* **1,** 7–28.

Meissner, R., 1996. Faults and folds, fact and fiction, *Tectonophysics,* **264,** 279–293.

Meissner, R. & Mooney, W., 1998. Weakness of the lower continental crust: a condition for delamination, uplift, and escape, *Tectonophysics,* **296,** 47–60.

Meissner, R. & Strehlau, J., 1982. Limits of stresses in the continental crust and their relation to depth-frequency distributions of shallow earthquakes, *Tectonics,* **1,** 73–89.

Meissner, R., Wever, T. & Sadowiak, P., 1991. Continental collision and seismic signature, *Geophys. J. Int.,* **105,** 15–23.

Mele, G., 1998. *Pn* anisotropy in the Northern Apennine Chain (Italy), *Pure appl. Geophys.,* **151,** 495–502.

Molnar, P.H. & Tapponier, P., 1975. Cenozoic tectonics of Asia: effects of continental collision, *Science,* **189,** 144–154.

Mooney, W.D. & Meissner, R., 1992. Multigenic origin of crustal reflectivity: a review of seismic reflection profiling of the continental lower crust and Moho in *Continental Lower Crust,* pp. 45–79, eds Fountain, D.M., Arculus, R. & Kay, R W., Elsevier, Amsterdam.

Montagner, J.-P. & Nataf, H.-C., 1986. A simple method for inverting the azimuthal anisotropy of surface waves, *J. geophys. Res.,* **91,** 511–520.

Montagner, J.-P., 1998. Where can seismic anisotropy be detected in the Earth's mantle? *Pure appl. Geophys.,* **151,** 223–256.

Nelson, K.D. *et al.*, 1996. Partially molten middle crust beneath southern Tibet: synthesis of project INDEPTH—results, *Science,* **274,** 1684–1688.

Nicolas, A. & Poirier, J.P., 1976. Crystalline plasticity and solid state flow in metamorphic rocks, Wiley, New York, p. 420.

Nicolas, A., Polino, R., Hirn, A., Nicolich, R. & ECORS-CROP working group, 1990. ECORS-CROP traverse and deep structure at the western Alps: a synthesis, *Mem Soc. geol. France, N.S.,* **156,** 15–27.

Nicolas, A. & Christensen, N.I., 1987. Formation of anisotropy in upper mantle peridotites—a review, *Rev. Geophys.,* **25,** 111–123.

Nolet, G. & Wortel, M.J.R., 1989. Mantle, upper: Structure, Encyclopedia, *Solid Earth Geophysics,* ed. James, D.E., von Norstrand Reinhold Co., New York.

Peselnik, L., Nicolas, A. & Stevenson, P.R., 1977. Velocity anisotropy in a mantle peridotite from the Ivrea zone. Application to upper mantle anisotropy, *J. geophys. Res.,* **79,** 1175–1182.

Porth, R., 2000. A strain-rate-dependent force model of lithospheric strength,*Geophys. J. Int.,* **141,** 647–660.

Plomerová, J., Liebermann, R.C. & Babuška, V., 1998. Geodynamics of the lithosphere and Earth's mantle: seismic anistropy as a record of the past and present dynamic processes, *Pure appl. Geophys.,* **151,** 213–218.
Rabbel, W., 1994. Seismic anisotropy at the continental deep drilling site (Germany), *Tectonophysics,* **232,** 329–341.
Rabbel, W. & Mooney, W., 1996. Seismic anisotropy of the crystalline crust: what does it tell us? Terra Research, *TerraNova,* **6,** 16–21.
Rabbel, W., Siegesmund, S., Weiss, T., Pohl, M. & Bohlen, T., 1998. Shear wave anisotropy of laminated lower crust beneath Urach (Germany): a comparison with xenoliths and with exposed lower crustal sections, *Tectonophysics,* **298,** 337–356.
Ranalli, G., 2000. Rheology of the crust and its role in tectonic reactivation, *J. Geodynam.,* **30,** 3–19.
Ratschbacher, L., Frisch, W., Neubauer, F., Schmid, S.M. & Neugebauer, J., 1989. Extension in compressional orogenic belts: the eastern Alps, *Geology,* **17,** 404–407.
Ribe, N.M., 1989. Seismic anisotropy and mantle flow, *J. Geophys.,* **94,** 4213–4223.
Russo, R.M. & Silver, P.G., 1998. Apparent shear wave splitting in the Nasca plate in the presence of vertically varying anisotropy, *Geophys. J. Int.,* **135,** 790–800.
Rutter, E.H. & Brodie, K.H., 1991. Lithospheric rheology—a note of caution, *J. Struct. Geol.,* **13,** 363–367.
Savage, M.K., 1999. Seismic anisotropy and mantle deformation: What have we learned from shear wave splitting? *Rev. Geophys.,* **37,** 165–106.
Schönenberg, R. & Neugebauer, J., 1987. Einführug in die Geologie Europas, pp. 1–294, Rombach Verlag, Freiburg.
Sengör, A.M., Yörur, N. & Saroglu, F., 1985. Strike-slip faulting and related basin formation in zones of tectonic escape: Turkey as a case study, *Spec. Publ. Soc. Econ. Palaeontol. Mineral.,* **37,** 227–264.
Sibson, R.M., 1982. Fault zone models, heat flow, and depth distribution of earthquakes in the continental crust of the United States, *Bull. seism. Soc. Publ. Soc. Econ. Palaeontol. Mineral.,* **72(1),** 1–163.
Siegesmund, S., 1996. The significance of rock fabrics for the geological interpretation of geophysical anisotropies, *Geotect. Forsch.,* **85,** 1–123.
Siegesmund, S. & Kern, H., 1990. Velocity anisotropy and shear-wave splitting in rocks from the mylonite belt along the Insubric Line (Ivrea Zone, Italy), *Earth palnet. Sci. Lett.,* **99,** 29–47.
Silver, P.G., 1996. Seismic anisotropy beneath the continents: probing the depth of geology, *Ann. Rev. Earth planet. Sci.,* **24,** 385–421.
Silver, P.G. & Chan, W.W., 1991. Shear wave splitting and subcontinental mantle deformation, *J. geophys. Res.,* **96,** 16 429–16 454.
Silver, P.G. & Savage, M., 1994. The interpretation of shear-wave splitting parameters in the presence of two anisotropic layers, *Geophys. J. Int.,* **119,** 949–963.
Smith, G.P. & Ekström, G., 1999. A global study of *Pn* anisotropy beneath continents, *J. geophys. Res.,* **104,** 963–980.
Stampfli, G.M., Masar, J., Marquer, D., Marchant, R., Baudin, T. & Barel, G., 1998. The tectonomorphic history of the peridotitic Chiavenna unit(Swiss Alps), *Tectonophysics,* **296,** 159–204.
Tapponier, P., Peltzer, G. & Amijo, R., 1986. On the mechanism of the collision between India and Asia, in *Collision Tectonics, Spec. Publ. Geol. Soc.,* Vol. 19,pp. 115–157, eds Coward, M.P. & Ries, A.C.
Tapponier, P., Peltzer, G., LeDain, A.Y., Armijo, R. & Coboöd, P., 1982. Propagating extrusion tectonics in Asia: new insight from simple experiments with plastiline, *Geology,* **10,** 611–616.
Tommasi, A., Tikoff, B. & Vauchez, A., 1999. upper mantle tectonics: three-dimensional deformation, olivine crystallographic fabrics and seismic properties, *Earth palnet. Sci. Lett.,* **168,** 173–186.
Vauchez, A., Barruol, G. & Nicolas, A., 1997. Why do continents break up parallel to ancient orogenic belts? *TerraNova,* **9(2),** 62–66.
Vauchez, A. & Nicolas, A., 1991. Mountain building: strike-parallel displacements and mantle anisotropy, *Tectonophysics,* **185,** 183–201.
Vauchez, A., Tommasi, A. & Barruol, G., 1998. Rheological heterogeneity, mechanical anisotropy and deformation of the continental lithosphere, *Tectonophysics,* **296,** 61–86.
Vetter, U. & Minster, J.B., 1981. *Pn* velocity anisotropy in southern California, *Bull. seism. Soc. Am.,* **71,** 1511–1530.
Vinnik, L.P., Makeyeva, L.I., Milev, A. & Usenko, A.Y., 1992. Global pattern of azimuthal anisotropy and deformations in the continental mantle, *Geophys. J. Int.,* **111,** 433–447.
Weertman, J., 1970. The creep strength of the earth's mantle, *Rev. Geophys. Space Phys.,* **8,** 145–168.
Weiss, T., Siegesmund, S., Rabbel, W., Bohlen, T. & Pohl, M., 1999. Seismic velocity and anisotropy of the lower continental crust: a review, *Pure appl. Geophys.,* **156,** 7–122.
Wendt, A., Mainprice, D., Rutter, E. & Wirth, T., 1998. A joint study of experimental deformation and experimentally induced microstructure of pretextured peridotites, *J. geophys. Res.,* **103,** 18 205–18 221.
Wenk, H.-R. & Tomé, C.N., 1999. Modelling dynamic recrystallization of olivine aggregates deformed in simple shear, *J. geophys. Res.,* **104,** 25 513–25 528.
Westaway, J., 1995. Crustal volume balance during the Indian–Asian collision and altitude of the Tibetan Plateau: a working hypothesis, *J. Geophys.,* **100,** 15 173–15 192.
Walter, C. & Flueh, E.R., 1993. The POLAR profile revisited: combined *P*- and *S*-wave interpretation, *Precambrian Res.,* **64,** 153–168.
Wysession, M.E., Fischer, K.M., Clarke, T.J., Al-eqapi, G.I., Fouch, M.J., Shore, P.J., Valenzuela, R.W. & Zaslow, J.M., 1996. Slicing into the Earth, *EOS, Trans. Am. geophys. Un.,* **477,** 480–482.
Yuan, X., Ni, J., Kind, R., Mechie, J. & Sandvol, E., 1997. Lithospheric and upper mantle structure of southern Tibet from a seismologocal passive source experiment, *J. geophys. Res.,* **102,** 27 491–27 500.
Yuan, X. *et al.*, 2000. Subduction and collision processes in the Central Andes, *Nature,* **408,** 958–961.
Zhao, W.L. & Morgan, W.J., 1987. Injection of Indian crust into Tibetan lower crust, *Tectonics,* **6,** 489–504.
Zoback, M.L., 1992. First and second-order patterns of stress in the lithosphere: the world stress map project, *J. geophys. Res.,* **97,** 11 703–11 727.
Zoback, M.L. *et al.*, 1989. Global patterns of tectonic stress, *Nature,* **341,** 291–298.

APPENDIX A: TOOTHPASTE-TUBE ESCAPE MODEL

In a general case, a flow of an incompressible viscous fluid with a constant viscosity η is specified by the Navier-Stokes equation and the equation of continuity:

$$-\nabla p + \rho g + \eta \Delta V = 0$$
$$\mathrm{div} V = 0 \tag{A1}$$

where p is hydrostatic pressure, ρ—fluid density, V—fluid velocity (Jaeger & Cook 1976). In a more general case of a depth-dependent viscosity they have the form:

$$-\frac{\partial P}{\partial x_i} + \frac{\partial}{\partial x_k}\left[\eta\left(\frac{\partial V_i}{\partial x_k} + \frac{\partial V_k}{\partial x_i}\right)\right] = 0$$
$$\frac{\partial V_l}{\partial x_l} = 0 \tag{A2}$$

with the summation over the repeated indices. Here $P = p - \rho g z$ is pressure generated by a fluid flow.

A horizontal flow of ductile material beneath mountain ridges can be explained within the framework of the following simple model. Consider a block with the horizontal dimensions W and L and the height H ($H \ll L$) (Fig. A1). Let rigid vertical walls approach each other with a constant velocity V_y in the direction normal to the walls (assume that the resulting variations of the initial distance

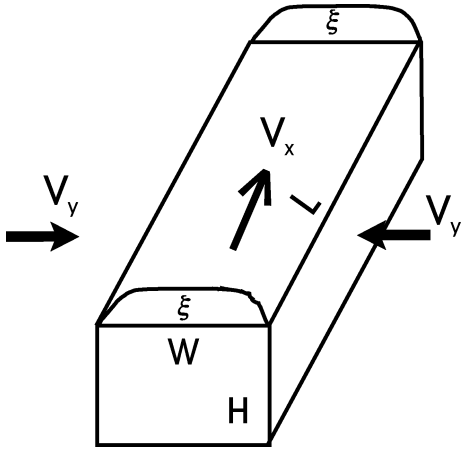

Figure A1. Block diagram of toothpaste-tube extrusion model. L, W, H = dimension of block (H ≪ L); V_y = velocity of approaching rigid boundaries; V_x = escape (extrusion) velocity.

W between them are small and $W \approx$ const). The condition $V_y =$ const means that an external pressure (force) at the approaching rigid boundaries is compensated by the excess hydrostatic pressure in a viscous fluid $\rho g \xi$, where ξ is the amplitude of the vertical distortion of the upper plane of the block due to the movement of its vertical boundaries. If $V_y =$ const, ξ should also be constant, $\frac{\partial P}{\partial y} = 0$, $\frac{\partial P}{\partial z} = 0$ and thus, the fluid in the system flows horizontally, free slip along the boundaries assumed. The velocity V_n be found from the mass balance and it depends on the amplitude ξ only through V_y:

$$V_x = V_y L / W. \tag{A3}$$

Eq. (A3) is identical to the solution of a 2-D problem for a fluid flow between two approaching rigid walls (Jaeger & Cook 1976) and remains valid for $\eta = \eta(z)$ for any z, i.e. depth distributions of $V_x(z)$ and $V_y(z)$ will have the same analytical expressions.

For a constant viscosity, the fluid (escape) velocity along the x-axis can be found from eq. (A1):

$$V_x \approx \frac{\rho g \xi}{\eta} \frac{1}{AL}, \tag{A4a}$$

where

$$A = \frac{1}{W^2} + \frac{1}{H^2} + \frac{1}{L^2}.$$

The constant velocity of the approaching walls is

$$V_y \approx \frac{\rho g \xi}{\eta} \frac{W}{AL^2} \tag{A4b}$$

The average expected escape velocity V_x is calculated from the observed values of plate convergence (DeMets *et al.* 1994) and the geometry of the specific mountain belt (the values of L, W, H). Table A1 contains the calculated values. Please note that we calculated the escape velocity twice: for the simple 2-D case (eq. A3) and for the 3-D case according to eq. (A4a) (last column) using average viscosity values of $10^{21}$and 10^{22} Pa s according to Fig. 1(b) (second last column) and various authors (e.g. Weertman 1970; Ranalli 2000; Porth 2000). We added the Proterozoic Trans-Hudson Orogen of the Canadian Shield for comparison. For this structure the convergence velocities are unknown; however, the escape velocities can be calculated if some assumptions are made for the values of the upper-mantle viscosity.

We are aware of the fact that our simple extrusion approach under the influence of lateral stresses does not take into account the dislocation of olivine minerals or its complex orientation or crystallisation as studied by Wenk & Tomé (1999) using plasticity theory. In our ductile 3-D model only the velocity of creep is calculated, and any orientation of anisotropic minerals will take place once the creep is established. No transpressional stresses and no vertical mantle faults are required (Tommasi *et al.* 1999). A significant result of our toothpaste tube model is the compatibility of our calculated (3-D) escape velocity with the observed escape—and convergence velocity when using well established and reasonable values for the (average) viscosity (from Fig. 1b). For Tibet, slightly higher values for the viscosity should be taken for calculating the estimated escape velocity. But in southern Tibet there is a massive introduction of (cold) Indian subcrustal lithosphere (Zhao & Morgan 1987; Kosarev *et al.* 1999; Kola-Ojo & Meissner 2001).

According to the concept of anisotropic viscosity, introduced by Christensen 1987 and Vauchez *et al.* (1997, 1998) we have used the minimum values (in the creep direction). They cover creep in the uppermost mantle and some contribution from the lower crust, but might also include higher values from a detached slab, like in Tibet and in the Alps, as was sketched in Fig. 2(b). However complex the single creep mechanism might be, we consider our toothpaste-tube model to be a simple and reasonable model for explaining the initiation of mountain-parallel creep in young orogens. Anisotropy is a consequence of the creep processes.

Table A1. Assessment of escape velocity V_x in 2-D (eq. A3) and 3-D (eq. A4a); Trans Hudson Orogen (1.8 Ga) for comparison.

Region	Convergence velocity V_y (cm y^{-1})	Width L (km)	Length W (km)	L/W	Escape velocity V_x 2-D (cm y^{-1}) (eq. A3)	Average viscosity in Pa s	Escape velocity V_x in 3-D (cm y^{-1}) (eq. A4a)
Tibet	5.0	2,000	1,000	2	10	10^{21}	5.0
						10^{22}	0.5
Turkey	1.0	800	500	1.6	1.6	10^{21}	2.4
						10^{22}	0.24
Alps	0.8	600	200	2.5	2.0	10^{21}	3.0
						10^{22}	0.3
Trans-Hudson	Unknown	2,000	1,000	2.0	Unknown	10^{21}	1.0
						10^{22}	0.1

Assuming viscosities of 10^{21} and 10^{22} Pa s, as in Fig. 1(a), the calculated escape velocities are similar to the convergence velocities and the observed escape velocities. This means that the assumed viscosities are realistic values.